Interference Force Reduction for Power Assist Systems Controlled at Arbitrary Operational Point

Fumiya Shibukawa
System Sensing and Control Laboratory, SSI
Hokkaido University, IST
Sapporo, Japan
shibukawa@ssc.ssi.ist.hokudai.ac.jp

Takayuki Tanaka, Shun'ichi Kaneko
System Sensing and Control Laboratory, SSI
Hokkaido University, IST
Sapporo, Japan
ttanaka;kaneko@ssi.ist.hokudai.ac.jp

***Abstract*— In this study, we propose an innovative multiportal human interface (M-HI) for power assist systems (PASs). This M-HI allows users to apply an operational force anywhere on the PAS. Because of this, the workspace of the PAS is extended and its end-effecter can be controlled as the user wishes. However, when users control a PAS at an intermediate joint, this joint does not always move in the same way as the end-effecter does. In this paper, we consider the number of links and degrees of freedom of a multilink manipulator. The relation between a control point and the limit of its motion is measured and analyzed. An operational position harmonization method is proposed through this relation. This method enables users to more accurately control the end-effector of a 3-link PAS at its intermediate joint.**

***Keywords*- Human robot interaction, User interfaces, Manipulator dynamics.**

I. Introduction

A. Background

No matter how large its workspace is, the area in which an ordinary power assist system (PAS) can operate is limited because of its restricted user motion space (see **Fig. 1(a)**). In addition, ordinary PAS requires the user to stay close to the target object. This situation may cause the object to catch on the user during motion, and may lead to a collision [5]. In this paper, we propose an innovative multiportal human interface (M-HI) [7]for PASs as a solution to these problems. M-HI enables users to control a PAS's end-effecter from anywhere on the system, and applying M-HI expands the effective workspace of a PAS, as shown in **Fig. 1(b)**. Thus, M-HI enables a user to control the PAS's end-effecter beyond the limitations of the human motion space.

During the control of a PAS, the user has some sense of the system's motion at the operational point. However, this motion is different from the actual end-effecter motion because of the degrees of freedom (DOFs) between the user and the end-effecter. Such differences are thought to affect the maneuverability and work accuracy of PASs.

Applying M-HI, therefore, carries the risk of reducing both maneuverability and user control sensitivity due to the difference between the operational force direction and operational point motion. Thus, controlling a PAS autonomously is necessary for not only tracing the user's operational force but also improving maneuverability. For example, in Koyama et al.'s research of HARO (a Human-Assisting Robot), the interference between a PAS and user caused by the mechanical construction of the system is reduced by using a filtering interference force method [4]. Kawamoto et al.'s HAL (Hybrid Assistive Leg)-3 [1], [3] PAS for gait disorder rehabilitation is controlled by estimating a user's intention from their myoelectric activity. In contrast, master-slave systems (MMSs) are not limited by the user's motion space. For example, Ishii's ASTACO (Advanced System with Twin Arms for Complex Operations) [2], Yokokohji's bilateral MMS [11] and Onal's bilateral MMS [6] enable

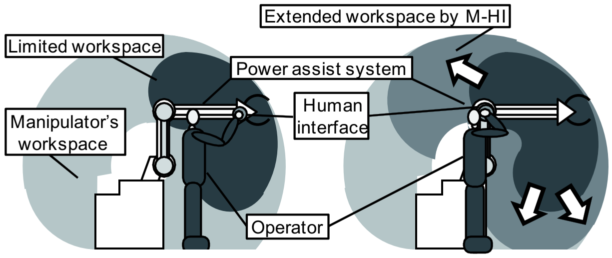

(a) Ordinary PAS (b) PAS with M-HI

Figure 1. Extending the workspace of a PAS by applying M-HI.

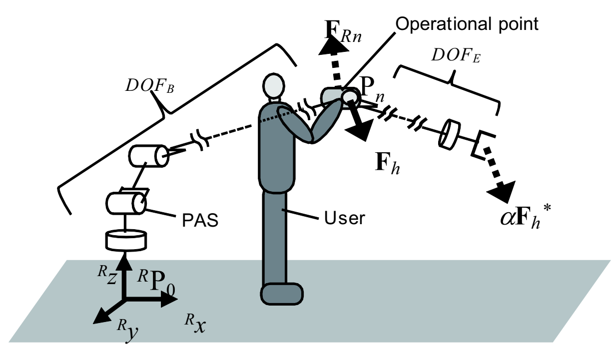

Figure 2. DOFs of PAS with M-HI and operational position force $\mathbf{F}_{Rn}$.

Copyright (c) IARIA, 2012. ISBN: 978-1-61208-232-5

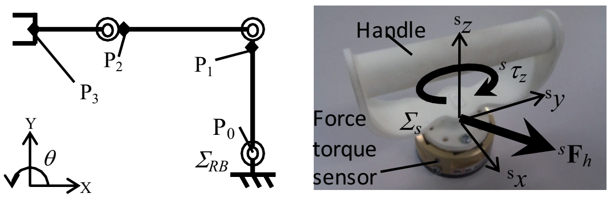

(a) Experimental PAS model (b) Force/torque sensor

Figure 3. Experimental PAS model.

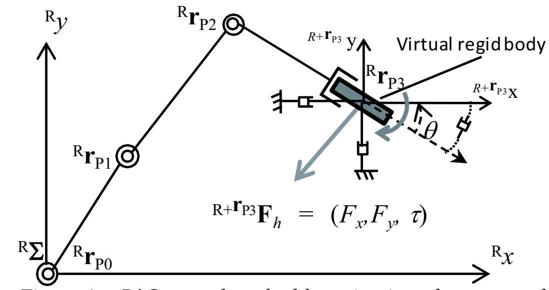

Figure 4. PAS control method by using impedance control.

the user to instinctively control the slave system by using a master system with the same DOFs. However, to realize such instinctive control, a high-specification master system is required.

For comparison, the characteristics that distinguish ordinary PAS, MSS and PAS with M-HI are as follows. In the proposed system, our M-HI technology enables the user to control the end-effecter's motion anywhere on the PAS and thus expands the effective workspace.

M-HI does not require a special master system. Moreover, by using an existing PAS and a force sensor, a system can be realized in which the user does not get needlessly close to target material. However, a PAS's end-effecter and other parts have different DOFs, and the force feedback is different for arbitrary operational points. These factors may strongly affect control sensitivity and accuracy. The conceptual model of our multilink PAS with M-HI is shown in **Fig. 2**.

The control response may become negative if the user's operational force $\mathbf{F}_h$ and the operational point force $\mathbf{F}_{Rn}$ are different. However, by following research such as Koyama et al. and Kawamoto et al., and controlling the PAS autonomously to fit to each individual situation, improvement of the PAS's maneuverability can be expected.

B. Purpose

We focus on the mutual interference between a PAS and user from the viewpoint of the force effect on the PAS by the user. We thus define the force as this effective force and experimentally analyze the relation between the user's operational force and operational point force.

In addition, we demonstrate the effectiveness of M-HI with respect to expanding the effective workspace of a PAS consisting of multi-DOF manipulators. An experiment applying M-HI to a 3-dof PAS, which limits the motion to the sagittal plane, is carried out, and the maneuverability of this system is evaluated. Controlling from an intermediate joint of the PAS, the motion of the control point sometimes has interference from the operational force. In this paper, we have two goals. Firstly, we try to measure and analyze the interference force betwen a user and an actual PAS. Secondly, we suggest a method to decrease the interference force and harmonize the control point force and operational force to improve maneuverability. We name this method 'operational point motion harmonization' (OPMH) and evaluate its effectiveness using computer simulation.

In this paper, the experimental condition and fundamental control method of M-HI are explained at next section. In the section three, fundamental operational force measurement and analysis are mentioned. In the fourth section, the improve method against operational force interference are proposed. In the fifth section, the method is evaluated. In the last saction, the paper is summarised.

II. APPLICATION OF M-HI TO 3-LINK PAS

A. Experimental setup

The experimental setup, PAS model and installed position force-torque sensor are shown in **Fig. 3**. In this experiment, we use a 3-link 3-DOF manipulator with the installed force/torque sensor as a PAS on $\mathrm{P}_1, \mathrm{P}_2$ or P_3. The PAS is moved by an impedance control method, where the motion is limited to the sagittal plane in this case.

B. 3-DOF PAS with impedance control

Our experimental 3-link PAS moved on impedance control method. The position and posture of 3-link PAS $\mathbf{r}_{\mathrm{P}_{3ref}} = [x_{3ref}, y_{3ref}, \theta_{3ref}]^T$ are calculated by the follow equation :

$$\mathbf{M}\frac{d^2\mathbf{r}_{\mathrm{P}_{3ref}}}{dt^2} + \mathbf{C}\frac{d\mathbf{r}_{\mathrm{P}_{3ref}}}{dt} = \alpha\mathbf{F}_h \tag{1}$$

This impedance method controls the PAS's motion by calculating the physical reaction of a virtual solid body [8], [10]. A user inputs an operational force and torque $\mathbf{F}_h(F_x, F_y, \tau)$ to the sensor attached to the PAS. The PAS's end-effecter motion is then calculated as the behavior of the virtual solid body given by Eq. (1). Here, $\mathbf{F}_h$ is the user's operational force, α is the assist ratio, $\mathbf{M}$ is the inertial matrix, $\mathbf{r}_{\mathrm{P}_{3ref}}$ is the position and orientation of the virtual solid body and $\mathbf{C}$ is a matrix of the system viscosities. The impedance control model of the 3-link PAS considering the end-effecter's position is shown in **Fig. 4**. According to the control method, the PAS's end-effector realizes the user's operational force.

Copyright (c) IARIA, 2012. ISBN: 978-1-61208-232-5

C. Application of M-HI for 3-link PAS

To apply M-HI, the operational force input to the end-effecter point must be estimated from the operational force given at an arbitrary operational point [7]. In this paper, this estimation is simply defined to make the evaluation of the proposed method straightforward:

$$\mathbf{F}_h^* = \mathbf{F}_h \tag{2}$$

Thus, we treat $\mathbf{F}_h$ and $\mathbf{F}_h^*$ as being the same from the basic viewpoint of the PAS's base. Using $\mathbf{F}_h^*$ as the operational force input to the end-effecter enables an arbitrary point control without changing the PAS's fundamental control system. In the next subsection, we discuss the motion DOFs of intermediate point control.

D. Motion limitations of arbitrary point control on a multilink system

If we wish to move the end-effecter through an arbitrary motion, the requirements to move with the desired motion are determined by the dimensions of the PAS's motion space while accounting for the solid body motion DOFs. When the PAS's motion space is one-dimension, the PAS only needs 1 DOF. When the PAS's motion space is two-dimensional, the PAS needs 2 DOFs for position and 1 DOF for orientation. When the PAS's motion space is three-dimensional, the PAS's needs 3 DOFs for position and 3 DOFs for orientation, specifically 6 DOFs in total [9]. We define the relation between a motion DOF and joint DOF of a PAS composed of a series of link manipulators by using Fig. 2. If the PAS moves in three-dimensional space, greater than 6 DOFs are required, those to realize the motion from the PAS's base to the user (DOF_B) and those from the user to the PAS's end-effecter (DOF_E). However, in this report, we do not treat such a complex manipulator, but instead our manipulator has a more limited number of DOFs. Therefore, DOF_B and DOF_E in our experimental setup are not enough to achieve free movement in three-dimensional space. In the next section, we discuss the maneuverability of the PAS with M-HI by considering the operational point force affect to the user.

III. Operational point interference force

A. Definition of operational point interference force

To evaluate the maneuverability of the PAS with M-HI, we consider the relation between the user's operational force $\mathbf{F}_h$ and the PAS's operational point force $\mathbf{F}_{Rn}$. This relation is determined by studying the position and orientation of the 3-DOF manipulator in which the motion space is limited to the sagittal plane. As a result, we see that the motion of the operational point is different from that of the PAS's end-effecter. For example, to achieve the motion in **Fig. 5** by controlling the PAS from the second link end P_2, the user must move the PAS's end-effecter position perpendicularly in the down direction and change its rotation counterclockwise as shown. According to Fig. 5, the operational point P_2 moves in the opposite direction to the operational force $\mathbf{F}_h$. The user has to control the PAS with a response $\mathbf{F}_{Rn}$ affected by the operational point. Hence, as an intuitive control for the PAS's end-effecter, we apply a method that realizes an amplified estimated operational force $\alpha\mathbf{F}_h^*$. However, this method is considered to decrease the operational sensitivity when the force caused by $\mathbf{F}_{Rn}$ differs from $\mathbf{F}_h$. We define the operational point interference force $\mathbf{F}_a$ through $\mathbf{F}_h$ and $\mathbf{F}_{Rn}$ as follows:

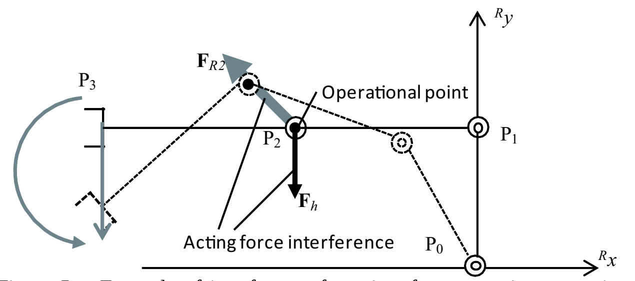

Figure 5. Example of interference force interference against operational force.

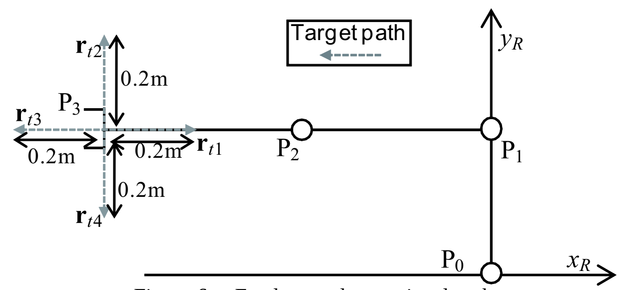

Figure 6. Fundamental operational paths.

$$\mathbf{F}_a = \mathbf{F}_{Rn} - \mathbf{F}_h \tag{3}$$

B. Experimental control accuracy of PAS with M-HI

We apply M-HI to an actual PAS and measure the control accuracy. In this experiment, we evaluate the tracking error of the PAS's end-effecter when controlled from an intermediate joint. During each trial, the user attempts to move the end-effecter to the target position. The user's control of the end-effecter motion is measured with the force/torque sensor, which is attached to P_3, P_2 or P_1, as shown in Fig. 3. The user inputs operational forces in the up, down, forward and backward directions, corresponding to $\mathbf{r}_{tn}, (n = 1 \cdots 4)$, respectively, until the end-effecter position moves by 0.2 m The user performs 10 repetitions in each direction. The target paths are shown in **Fig. 6**. The evaluation criterion, the target

Copyright (c) IARIA, 2012. ISBN: 978-1-61208-232-5

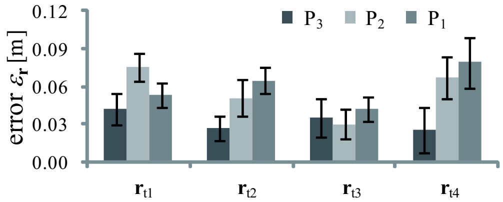

Figure 7. Experimental operational accuracy of PAS with M-HI.

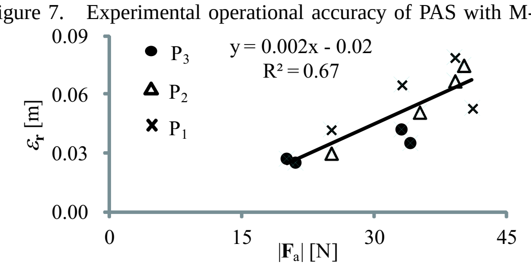

Figure 8. Correlation between average operational point interference force $|\bar{\mathbf{F}}_a|$ and control accuracy $\varepsilon_{\mathbf{r}}$.

path tracking error, is defined by follow equation:

$$\varepsilon_{\mathbf{r}} = \frac{1}{N_s}\sum_{i=0}^{N_s}\sqrt{|^{\mathrm{P}_{e0}}\mathbf{r}_{\mathrm{P}_{3_i}}|^2 - \frac{(^{\mathrm{P}_{e0}}\mathbf{r}_{\mathrm{P}_{3_i}} \cdot {}^{\mathrm{P}_{e0}}\,\mathbf{r}_{t_n})^2}{|^{\mathrm{P}_{e0}}\mathbf{r}_{t_n}|^2}} \qquad (4)$$

Here, P_{e0} means intitial end-effecter positon, $\mathbf{r}_{t_n}$ is position of the target path, $\mathbf{r}_{P_{3_i}}$ is end-effecter position on the coordinate of P_{e0} and N_s is the total step count. According to Eq. (4), a small value of $\varepsilon_{\mathbf{r}}$ indicates a small error between the end-effecter and target paths. The experimental results are shown in **Fig. 7**. Compared with P_3 control, both P_1 and P_2 controls have large target path tracking errors $\varepsilon_{\mathbf{r}}$. We have thus verified the decrease in control accuracy of the PAS with M-HI. The relation between the average interference force $|\bar{\mathbf{F}}_a|$ and control accuracy $\varepsilon_{\mathbf{r}}$ is shown in **Fig. 8**. Analysis of these data show that the correlation coefficient is 0.76, and we have therefore also verified the correlation between tracking error and $|\bar{\mathbf{F}}_a|$. These results infer that control accuracy improvement can be expected by reducing the operational force interference. We now propose a maneuverability improvement method that takes account of this operational force interference.

IV. Operational point motion harmonization

We propose a method to reduce the interference force interference and to harmonize this force and the operational position. We term this method "operational point motion harmonization control (OPMH)". OPMH has two goals; firstly, to reduce the interference force on the operational point, and secondly, to minimize the end-effecter motion error. A schematic of the OPMH control algorithm is shown in **Fig. 9**, and the operational force interference reduction algorithm is shown in **Fig. 11**. Here, the difference $\mathbf{F}_a$ is thought of as the correction force of the operational point motion that must be added alongside $\mathbf{F}_{Rn}$. If the operational point moves due to the combination of the correction force

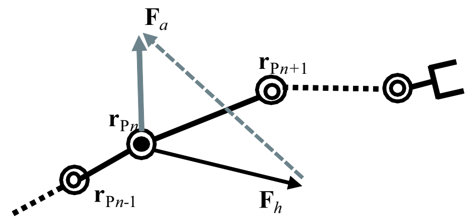

Figure 9. Definition of the interference force $\mathbf{F}_a$.

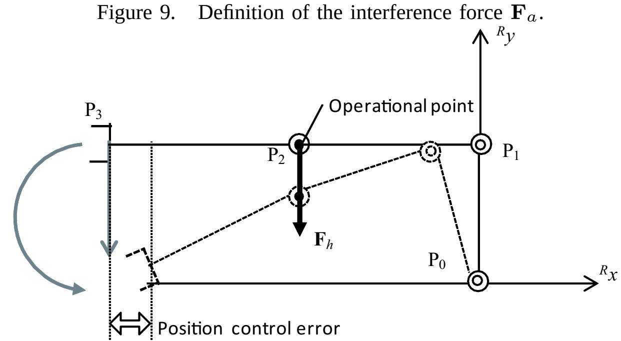

Figure 10. Example of position control error caused by canceling interference force.

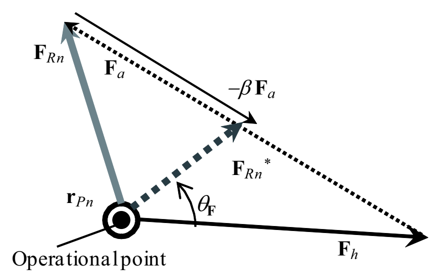

Figure 11. Concept of operational point motion harmonization.

and $\mathbf{F}_{Rn}$, then the motion is the same as that due to $\mathbf{F}_h$. However, the end-effecter motion will be different from that calculated by the impedance control method. For example, if 3 DOF PAS with M-HI as seen **Fig. 10** controlled P_2 following the operational force $\mathbf{F}_h$, P_3 motion has some errors compared with the motion calculated by impedance model. Therefore, we define the product of the correction force and β as the OPMH force $\beta\mathbf{F}_a$, which then gives the modified operational point force $\mathbf{F}^*_{Rn}$ as follows:

$$\mathbf{F}^*_{Rn} \quad = \quad \beta\mathbf{F}^*_h + (1-\beta)\mathbf{F}_{Rn} \qquad (5)$$

According to the above definition, if β is close to 1, then the operational point motion is close to that given by the operational force. By optimizing β, we can reduce both the interference force interference at the operational point and the end-effecter motion error. Thus M-HI enables the user to accurately control the PAS's end-effecter from anywhere on the PAS. The control flow of OPMH, including β optimization, is shown in **Fig. 12**. The evaluation function V for optimizing the system is defined as follows:

$$V \quad = \quad V_f + V_p \qquad (6)$$

Copyright (c) IARIA, 2012.

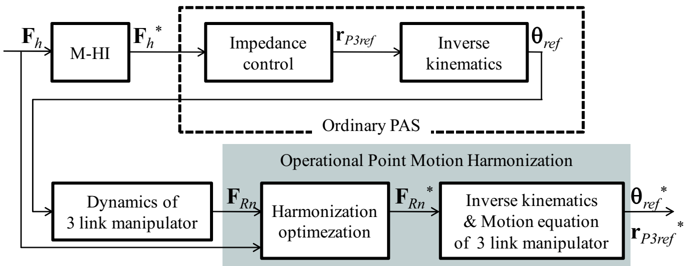

Figure 12. Block diagram of OPMH.

Here, V_f denotes the effect of operational interference and V_p denotes the error of the end-effecter motion resulting from the impedance model. V_f and V_p are given by follow equations.

$$V_f = 0.5\cos(\theta_{\mathbf{F}} + 1) \tag{7}$$

$$\theta_{\mathbf{F}} = \cos^{-1}\left(\frac{\mathbf{F}_{Rn}^* \cdot \mathbf{F}_h}{|\mathbf{F}_{Rn}^*||\mathbf{F}_h|}\right) \tag{8}$$

$$V_p = 0.5\cos(\theta_P + 1) \tag{9}$$

$$\theta_P = \cos^{-1}\left(\frac{\Delta\mathbf{r}_{\mathrm{P}_3}^* \cdot \Delta\mathbf{r}_{\mathrm{P}_{3ref}}}{|\Delta\mathbf{r}_{\mathrm{P}_3}^*||\Delta\mathbf{r}_{\mathrm{P}_{3ref}}|}\right) \tag{10}$$

$$\Delta\mathbf{r}_{\mathrm{P}_3}^* = \mathbf{r}_{\mathrm{P}_3}^*(t+\Delta t) - \mathbf{r}_{\mathrm{P}_3}(t) \tag{11}$$

$$\Delta\mathbf{r}_{\mathrm{P}_{3ref}} = \mathbf{r}_{\mathrm{P}_{3ref}}(t+\Delta t) - \mathbf{r}_{\mathrm{P}_3}(t) \tag{12}$$

Here, $\Delta\mathbf{r}_{\mathrm{P}_{3ref}}$,$\Delta\mathbf{r}_{\mathrm{P}_3}^*$ means amounts of change of P_{3ref} and P_3^* position, and their definition are shown in **Fig. 14**. V is minimized through optimization of β. In Eq. (7), V_f is changed between 0 and 1 by the direction of $\mathbf{F}_a$. In Eq. (9), V_p is changed between 0 and 1 by the direction that gives a decrease in the end-effecter motion error resulting from the reduction of $\mathbf{F}_a$. Hence, OPMH optimizes β such that V is minimized through V_f and V_p. If V_f takes precedence, then β becomes close to 1, and if V_p takes precedence, then β becomes close to 0. Examples of each evaluation function during the controlling of PAS with M-HI and applying OPMH are shown in **Fig. 13**. In this experiment, β is optimized by the following method. During a step controlling the PAS with M-HI, β is changed from 0.00 to 1.00 in increments of 0.01. In each β, the evaluation function V is calculated. The β which has the smallest V is chosen as the optimized β in this controlling step. We see a clear change in β from 0 to 1 dependent on the values of V_f and V_p. The definitions of $\Delta\mathbf{r}_{\mathrm{P}_{3ref}}^* and \Delta\mathbf{r}_{\mathrm{P}_{3ref}}$ are shown in Eq. (12),(11) and **Fig. 14**. Here, Δt represents the time during a step calculating the PAS motion and moving the PAS.

V. Evaluation of OPMH

We evaluate the effect of OPMH by using both a computer simulation to remove individual variation of experimental motions and guarantee repeatability. We evaluate the effect of OPMH through computer simulation by examining the

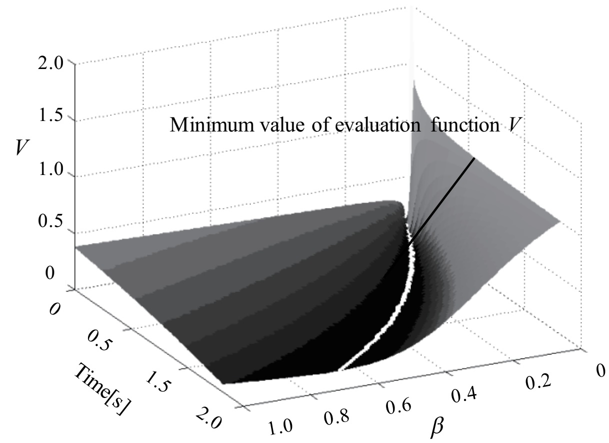

Figure 13. Example of β optimization.

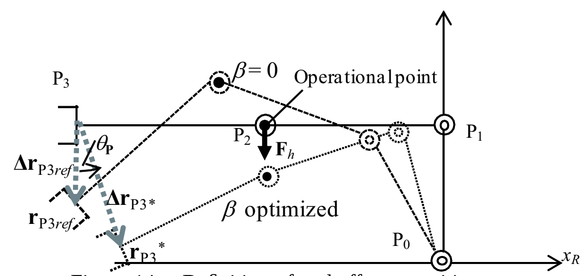

Figure 14. Definition of end-effecter position error.

control accuracy and interference force. Following the experiment in Section 3, the user inputs an operational force $\mathbf{F}_h$ to the four targets $\mathbf{r}_{t1\cdots4}$ shown in Fig. 6. In the current experiment, the absolute value of $\mathbf{F}_h$ increases from 10 to 40 N in 10 N intervals, and we evaluate the operational point interference force and the end-effecter tracking error.

A. Interference force $\mathbf{F}_a$ reduction

We verify the interference force reduction effect of applying OPMH by using the average interference force $|\bar{\mathbf{F}}_a|$ during a trial as defined by the follow equation:

$$|\bar{\mathbf{F}}_a| = \frac{1}{N_s}\sum_{i=0}^{N_s}\Big(|\mathbf{F}_{Rn_i} - \mathbf{F}_{h_i}|\Big) \tag{13}$$

The experimental results are shown in **Fig. 15**. In these figures, $\beta = 0$, $\beta = 1$ and β is optimized denote the respective cases of not considering the interference force, completely canceling out the interference force and applying OPMH with β optimization considering the interference force and end-effecter motion error. Fig. 15 shows the $|\bar{\mathbf{F}}_a|$ compared by $|\mathbf{F}_h|$ under the target path $\mathbf{r}_{t4}$. We can see that the interference force $|\bar{\mathbf{F}}_a|$ is increased by increasing the operational force $|\mathbf{F}_h|$. However, irrespective of the magnitude of $|\mathbf{F}_h|$, $|\bar{\mathbf{F}}_a|$ is decreased by applying OPMH. $|\bar{\mathbf{F}}_a|$ reduction ratio was 16.3% at P_1 and 19.1% at P_2.Therefore, we confirmed the interference force $\mathbf{F}_a$ reduction by OPMH.

Copyright (c) IARIA, 2012. ISBN: 978-1-61208-232-5

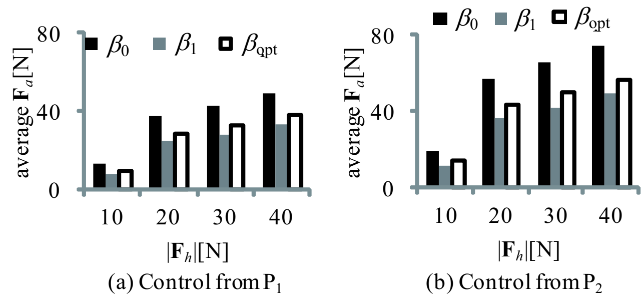

Figure 15. Average interference force from simulations under the target path $\mathbf{r}_{t4}$.

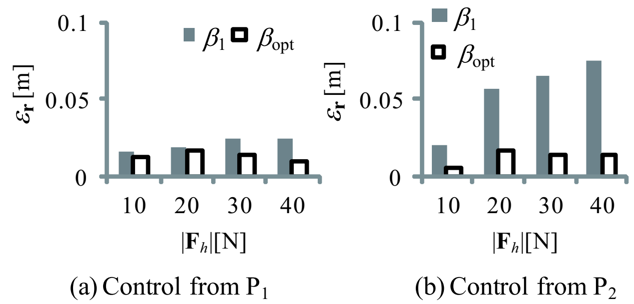

Figure 16. Average end-effecter position error of simulations under the target path $\mathbf{r}_{t4}$.

B. Target path tracking error

Next, we evaluate the motion error of PAS's end-effecter caused by applying OPMH. The motion error of PAS's end-effecter is calculated by Eq. (4). The experimental results are shown in **Fig. 16**. Here, the simulations of the case when $\beta = 0$ are not plotted since $\mathbf{F}^*_{Rn} = \mathbf{F}_{Rn}$ and hence $\varepsilon_{\mathbf{r}} = 0$ from Eqs. (5) and (4). Fig. 16 shows $\varepsilon_{\mathbf{r}}$ compared by $\mathbf{F}_h$ under the target path $\mathbf{r}_{t4}$. According to the figure, $\varepsilon_{\mathbf{r}}$ values under the optimized β is less than the values under the $\beta = 1.0$ as we had expected. The error of the end-effecter when position tracking to the target path was 23.8% at P_1 and 60.6% at P_2.According to this result, an improvement in control accuracy is found by using OPMH and its parametar β optimization. The experimental resulats of $|\bar{\mathbf{F}}_a|$ and $\varepsilon_{\mathbf{r}}$ shows that the PAS with M-HI applied OPMH move canceling $\mathbf{F}_a$ with minimum P_3 motion error. Therefore OPMH is expected the improvement of operational feelings with the minimum P_3control accuracy loss.

VI. Conclusion

In this report, we applied M-HI to a 3-link PAS. We defined the force affected by the PAS's operational point as the interference force and analyzed the interference phenomenon of this force. We proposed OPMH as a method for reducing the interference force interference and for tracing the user's operational force. We evaluated the effects of OPMH by computer simulation. From the experimental results, we have shown the improvements in operational accuracy and efficiency of applying OPMH to the PAS with M-HI. Regarding operational accuracy, the error of the end-effecter when position tracking to the target path was 23.8% at P_1 and 60.6% at P_2.According to experimental result, OPMH is expected the improvement of operational feelings with the minimum control accuracy loss as we had expected. Therefore, we confirmed the effectiveness of OPMH applying PAS with M-HI.

References

[1] T. Hayashi, H. Kawamoto, and Y. Sankai. "Control method of robot suit HAL working as operator's muscle using biological and dynamical information". *Proc. of IEEE/RSJ International Conference on Intelligent Robots and Systems*, pp. 3063–3068, Aug 2005.

[2] A. Ishii. "Operating System of a Double-Front Work Machine for Simultaneous Operation". *Proc. of Int. Symp. Automation and Robotics in Construction*, pp. 539–542, 2006.

[3] H. Kawamoto and Y. Sankai. "Power Assist System HAL-3 for Gait Disorder Person". *Proc. of the 8th Int. Conf. on Computers Helping People with Special Needs*, pp. 196–203, 2002.

[4] T. Koyama, M. Q. Feng, and T. Tanaka. "Development and Motion Control of a Wearable Human Assisting Robot for Nursing Use". *Human Friendly Mechatronics(ICMA 2000)*, pp. 105–110, 2001.

[5] A. E. McMichael. "Army Materiel Handling Accident Analysis ". *Proc. of the Human Factors Society 32nd Annual Meeting 1988*, pp. 889–891, 1988.

[6] C. D. Onal and A. Sabanovic. "Bilateral control with a reflex mechanism on the slave side". *Proc. of Industrial Electronics Society 31st Annual Conference of IEEE*, pp. 849–852, Nov 2005.

[7] F. Shibukawa, T. Tanaka, and S. Kaneko. "Multi-portal Human Interface". *Proc. of the Int. Conf. IEEE Industrial Electronics*, pp. 4259–4264, 2009.

[8] T. Tsuji, H. Akamatsu, K. Harada, and M. Kaneko. "On-line Learning of Rob ot Arm Imp edance Using Neural Networks". *Journal of Robotics Society of Japan*, Vol. 17, No. 2, pp. 234–241, 1999.

[9] K. Yamane and N. Yoshihiko. "Pin-and-Drag Synergetic Interface for Choreography of Human Figures". *Journal of Robotics Society of Japan*, Vol. 20, No. 3, pp. 335–343, 2002.

[10] I. Yasuyuki, S. Tachi, and H. Arai. "A Method of Impedance Control of a Master-slave Manipulation System". *Journal of Robotics Society of Japan*, Vol. 10, No. 4, pp. 490–500, 1992.

[11] Y. Yokokohji. "Bilateral Control of Master-slave Manipulators for Ideal Kinesthetic Coupling". *Proc. of IEEE Int. Conf. Robotics and Automation*, pp. 849–852, 1992.

Copyright (c) IARIA, 2012. ISBN: 978-1-61208-232-5